IEEE Access
Multidisciplinary | Rapid Review | Open Access Journal

Received May 29, 2018, accepted July 3, 2018, date of publication July 11, 2018, date of current version December 31, 2018.

Digital Object Identifier 10.1109/ACCESS.2018.2854227

Transient Stability Assessment Using Individual Machine Equal Area Criterion PART I: Unity Principle

SONGYAN WANG, JILAI YU, AND WEI ZHANG, (Member, IEEE)
School of Electrical Engineering and Automation, Harbin Institute of Technology, Harbin 150001, China
Corresponding author: Songyan Wang (wangsongyan@163.com)

ABSTRACT Analyzing the system trajectory from the perspective of individual machines provides a distinctive approach for the analysis of the transient stability of power systems. These two-paper series propose a direct-time-domain method that is based on the individual-machine equal area criterion. In the first paper, by examining the mapping between the trajectory and power-vs-angle curve of an individual machine, the stability property that characterizes a critical machine is elucidated. The mapping between the system trajectory and the individual-machine equal area criterion is established. Furthermore, a unity principle between the individual-machine stability and system stability is proposed. It is proved that the instability of the system can be confirmed by finding any one unstable critical machine, enabling the monitoring of the transient stability of a multimachine system in an individual-machine manner in transient stability assessment.

INDEX TERMS Transient stability, equal area criterion, individual machine energy function, partial energy function.

NOMENCLATURE

COI	Center of inertia
CCT	Critical clearing time
DLP	dynamic liberation point
DSP	dynamic stationary point
EAC	Equal area criterion
IMT	Individual-machine trajectory
PEF	Partial energy function
TSA	Transient security assessment
UEP	Unstable equilibrium point
3DKC	3-dimensional Kimbark curve
CDSP	DSP of the critical stable machine
CUEP	Controlling UEP
EEAC	Extended EAC
IMEF	Individual machine energy function
IVCS	Individual machine-virtual COI machine system
LOSP	Loss-of-synchronism point
OMIB	One-machine-infinite-bus
SIME	Single machine equivalence
IEEAC	Integrated EEAC
IMEAC	Individual-machine EAC

I. INTRODUCTION

A. LITERATURE REVIEW

In the last several decades, intense efforts have been made to apply transient stability analysis in power system operation [1]. Power system transient stability is typically assessed either through time-domain simulation or through transient energy methods. In recent years, in the field of time domain simulation, the high-speed transient stability simulation and parallel simulation techniques have made real-time simulations of large-scale power networks feasible [2], [3]. Trajectory sensitivity methods based on time domain simulations are used in the determination of power flow limits and dynamic Var planning [4], [5]. In addition, the use of some novel pattern recognition techniques that rely on phasor measurement units is also becoming a promising approach for predictions of the transient stability status of power systems [6].

Compared to the time domain simulation, transient energy methods or direct methods also play an important role in power system transient stability analysis because these methods are advantageous for describing the system's ability

to absorb the fault-on energy during the post-fault period. In early work, the Lyapunov method was demonstrated to yield conservative results. Since then, direct methods such as the CUEP method, the sustained fault method and the EEAC method have received considerable attention and achieved significant advances [7], [8]. These methods monitor transient behaviors of all machines in the system in TSA and are also known as global methods. Recently, with the increasing penetration of renewable power plants and plug-in hybrid electric vehicles, some novel application of the global methods, such as the integration of the global transient energy function and recloser probability distribution functions, have also been developed to provide a quantitative measure of probability of stability [9].

Interestingly, unlike the global methods described above that show good performance in transient stability analysis, a few direct methods study the power system transient stability from the distinctive individual-machine standpoint because "the instability of a multi-machine system is determined by the motion of some unstable critical machines if more than one machine tends to lose synchronism" [10], [11]. Stimulated by this individual-machine perspective, Vittal [12] and Fouad *et al.* [13] stated that the instability of the system depends on the transient energy of the individual machines, and IMEF was proposed. Stanton [14]–[16] performed a detailed machine-by-machine analysis of a multi-machine instability, and PEF was used to quantify the energy of a local control action. Later, EAC of the critical machine was applied in the PEF method to identify system stability [17]. Rastgoufard *et al.* [18] used a synchronous referred IMEF to determine the transient stability of a multimachine system. Haque [19] proposed an efficient individual-machine method to compute the CCT of the system under transients. Ando and Iwamoto [20] also presented a potential energy ridge, which can be used to predict the single-machine stability. Generally, among all of these individual-machine studies, the IMEF method and PEF method are quite representative and can be viewed as milestones in the history of the development of the individual-machine methods because they initially explained the fundamental structures, theories and provided a quite valuable underlying hypothesis. Although individual-machine methods were initially proved to be effective for transient stability analysis, these methods have been at a standstill in recent years. This is because the research of some crucial concepts of the individual-machine methods has been suspended. Key questions encountered by global analysts can be described as below:

(i) How to identify the stability of an individual machine?

(ii) What is the relationship between the individual machine stability and system stability?

(iii) How to apply individual-machine method in the industrial large scale network?

These unsolved questions made individual-machine methods quite controversial compared with global methods. Among all these questions, (ii) is most widely questioned by global analysts [15], [16]. Therefore, it is worthy to propose a novel individual-machine approach to solve the problems above, which may contribute to a new understanding about power system transient stability in an individual-machine manner.

B. SCOPE AND CONTRIBUTION OF THE PAPER

This two-paper series can be seen as clarification, correction and extension of the classic individual machine methods [13]–[20]. Our work aims to propose a novel direct-time-domain individual-machine method that can be applied in TSA of the actual industrial network. The first paper systematically elucidates the mechanism of the proposed method in the monitoring of the transient stability of a multi-machine system (for Questions (i) and (ii)). The companion paper applies the proposed method for TSA and CCT computation (for Question (iii)). In the first paper, based on the actual trajectory of the system trajectory during the transients, the Kimbark curve of a critical machine is first analyzed, and then the individual-machine equal area criterion (IMEAC) is proved to strictly hold for a critical machine. Second, following the trajectory stability theory, the concept of individual-machine trajectory (IMT) is proposed, and the mapping between the system trajectory and the Kimbark curve of an individual machine is established. Finally, the unity principle relationship between the individual-machine stability and system stability is proposed. It shows that IMT of any one unstable critical machine can drive the system trajectory to become unstable so that the transient stability of a multi-machine system can be monitored in an individual-machine manner during TSA.

The contributions of this paper are summarized as follows:

(i) The stability characterization of a critical machine is depicted via IMEAC. The proposed method is essentially different from the group-separation based IEEAC method, which provides an alternative way for power system transient stability analysis;

(ii) Mistakes regarding the stability characterization of a critical machine in [15] and [16] are corrected in this paper. This eliminates misunderstanding about the stability characterization of a critical machine existed in the previous works;

(iii) The unity principle explicitly describing the relationship between the individual-machine stability and system stability is proposed. This provides a potential that power system transient stability can be analyzed nonglobally.

In this paper, a critical machine is defined as the machine with advanced angle during the post-fault transient period [10], [11]. We only discuss the first-swing stability of a critical machine, and the swing stability in this paper only depicts the stability state of a critical machine when the velocity of the machine reaches zero, rather than following the conventional global concept.

Three test systems are applied in this two-paper series. Test System-1 (TS-1) is a modified IEEE 39-bus system. In TS-1, the inertia constant of Unit 39 is modified to 200 p.u. from 1000 p.u.; Test System-2 (TS-2) is the standard

IEEE 118-bus system. Test System-3 (TS-3) is a practical 2766-bus interconnected system. All faults are three phase short-circuits faults, which occurred at 0 *s* and are cleared without line switching. Fault types in this two-paper series are described in the form of [test-system, fault location, fault-on time]. The simulations of TS-1 and TS-2 are fully based on the classical model given in [13]. The simulations of TS-3 are based on complicated dynamic models, and the parameters of this system can be found in the companion paper.

The rest of the paper is organized as follows. In Section II, IMEAC of a critical machine is analyzed. In Section III, the Kimbark curves of both critical machines and non-critical machines that rely on the actual system trajectory in the multi-machine system are analyzed. In Section IV, the mapping between IMT and the Kimbark curve of a critical machine is established. In Section V, the unity principle of the stability of the system and that of a critical machine is described in the sense of IMT. In Section VI, a tutorial example for the application of the proposed method in TSA is demonstrated. Conclusions are stated in Section VII.

II. INDIVIDUAL MACHINE EQUAL AREA CRITERION

A. EQUATION OF MOTION OF AN INDIVIDUAL MACHINE

Conventionally, for a direct method based on the COI reference, ''an individual machine'' should be precisely expressed as ''an individual machine in COI reference''. For a n-machine system with rotor angle δ_i and inertia constant M_i, the motion of an individual machine i in the synchronous reference is governed by the differential equations

$$\begin{cases} \dot{\delta}_i = \omega_i \\ M_i\dot{\omega}_i = P_{mi} - P_{ei} \end{cases} \tag{1}$$

The position of the COI of the system is defined by

$$\begin{cases} \delta_{COI} = \dfrac{1}{M_T}\sum_{i=1}^{n} M_i\delta_i \\ \omega_{COI} = \dfrac{1}{M_T}\sum_{i=1}^{n} M_i\omega_i \\ P_{COI} = \sum_{i=1}^{n}(P_{mi} - P_{ei}) \end{cases} \tag{2}$$

where $M_T = \sum_{i=1}^{n} M_i$.

From Eq. (2), the motion of COI is determined by

$$\begin{cases} \dot{\delta}_{COI} = \omega_{COI} \\ M_T\dot{\omega}_{COI} = P_{COI} \end{cases} \tag{3}$$

Eq. (3) indicates that COI can also be seen as a virtual ''machine'' with its own equation of motion described as the aggregated motion of all machines in the system. The trajectory of the virtual COI machine in synchronous reference is shown in Fig. 1.

Since machine i and COI are two ''individual'' machines with interactions, a two-machine system named as individual machine-virtual COI machine system (IVCS) can be formed by these two machines, as illustrated in Fig. 2. The relative trajectory between a critical machine and the virtual COI machine in an IVCS is shown in Fig. 3.

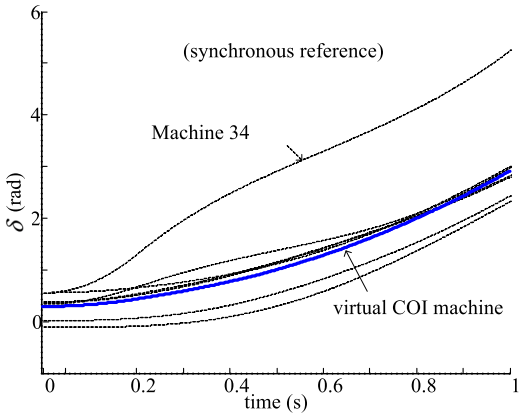

FIGURE 1. Trajectory of the virtual COI machine [TS-1,bus-34, 0.202s].

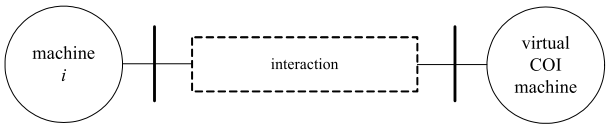

FIGURE 2. Two-machine system formed by machine *i* and virtual COI machine.

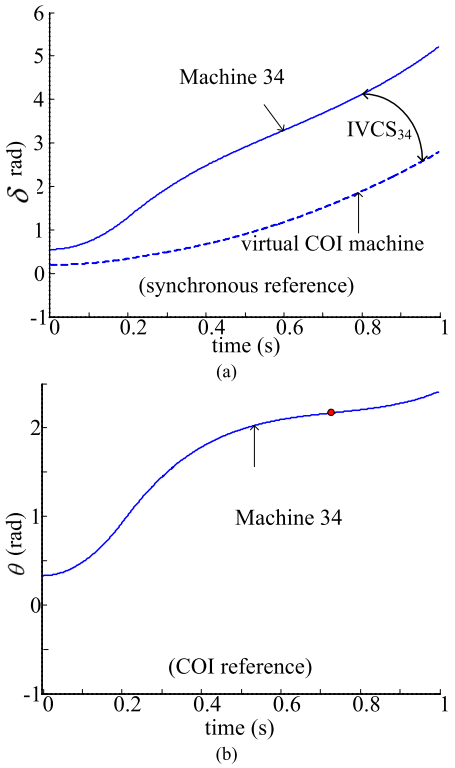

FIGURE 3. Instability of the relative trajectory between a critical machine and the virtual COI machine [TS-1, bus-34, 0.202s]. (a) IVCS in synchronous reference. (b) individual machine in COI reference.

Following (1) and (3), the relative motion between machine i and the virtual COI machine in an IVCS can be denoted as

$$\dot{\theta}_i = \tilde{\omega}_i, \quad M_i\dot{\tilde{\omega}}_i = f_i \tag{4}$$

where

$$f_i = P_{mi} - P_{ei} - \frac{M_i}{M_T} P_{COI}$$
$$\theta_i = \delta_i - \delta_{COI}$$
$$\tilde{\omega}_i = \omega_i - \omega_{COI}$$

Eq. (4) depicts the separation of an individual machine with respect to the COI of all machines in the system, which is essentially identical to the motion of an individual machine in the COI reference. Therefore, each individual machine in the COI reference should be precisely depicted as an IVCS formed by a "pair" of machines. However, in this paper, for historical reasons, the "individual machine" or "critical machine" is still used as a default term for simplification to represent the pair of the machines.

B. STRICT EAC CHARACTERISTIC OF AN INDIVIDUAL MACHINE

Since EAC only strictly holds in the one-machine-infinite-bus (OMIB) system and the two-machine system, the analysis in Section A is valuable because it indicates that EAC strictly holds for an individual machine as the IVCS is a precise two-machine system.

Following Eq. (4), we have

$$f_i d_{\theta_i} = M_i \tilde{\omega}_i d_{\tilde{\omega}_i} \tag{5}$$

Along the actual fault-on trajectory until fault clearing, we have

$$\int_{\theta_i^0}^{\theta_i^c} f_i^{(F)} d_{\theta_i} = \int_{\tilde{\omega}_i^0}^{\tilde{\omega}_i^c} M_i \tilde{\omega}_i d_{\tilde{\omega}_i} \tag{6}$$

where $f_i^{(F)}$ corresponds to f_i during the fault-on period.

Eq. (6) can be further expressed as

$$\frac{1}{2} M_i \tilde{\omega}_i^{(c)2} = \int_{\theta_i^0}^{\theta_i^c} \left\{ 0 - (-f_i^{(F)}) \right\} d_{\theta_i} \tag{7}$$

Along the actual post-fault trajectory after fault clearing, we have

$$\int_{\theta_i^c}^{\theta_i} f_i^{(PF)} d_{\theta_i} = \int_{\tilde{\omega}_i^c}^{\tilde{\omega}_i} M_i \tilde{\omega}_i d_{\tilde{\omega}_i} \tag{8}$$

where $f_i^{(PF)}$ corresponds to f_i during post-fault period.

Eq. (8) can be further expressed as

$$\frac{1}{2} M_i \tilde{\omega}_i^{(c)2} = \frac{1}{2} M_i \tilde{\omega}_i^2 + \int_{\theta_i^c}^{\theta_i} \left\{ -f_i^{(PF)} - 0 \right\} d_{\theta_i} \tag{9}$$

Substituting (7) in (9) yields

$$\int_{\theta_i^0}^{\theta_i^c} \left\{ 0 - (-f_i^{(F)}) \right\} d_{\theta_i} = \frac{1}{2} M_i \tilde{\omega}_i^2 + \int_{\theta_i^c}^{\theta_i} \left\{ -f_i^{(PF)} - 0 \right\} d_{\theta_i} \tag{10}$$

A typical Kimbark curve [16] (power-vs-angle curve) of an unstable critical machine formulated with the actual simulated system trajectory in the $\theta_i - f_i$ space is shown in Fig. 4(a). The rotor angles of the system are shown in Fig. 4(b).

We assume that the Kimbark curve of the machine reaches the liberation point (P3) as shown in Fig. 4. In this case, both of the integrals in Eq. (10) can be viewed as "areas", and the difference between the acceleration area and the deceleration area is the residual "K.E." of the machine at the liberation point (P3). Therefore, the machine can be evaluated as unstable as long as the acceleration area is larger than the deceleration area (i.e., the residual K.E. is positive at the liberation point), and the machine can be evaluated as stable if the acceleration area is equal to the deceleration area (i.e., the residual K.E. is strictly zero at the liberation point). This fully proves that *EAC strictly holds for an individual machine*.

In power system transient stability analysis, critical machines are the few severely disturbed machines that are most likely to separate from the system, while non-critical machines are the slightly disturbed machines which oscillate during the post-fault period. Therefore, the transient behavior and corresponding Kimbark curve of a critical machine will be quite different from those of a non-critical machine. In the following work, the first task is to analyze the transient characteristic of the Kimbark curve of an individual machine because such analysis may reveal the fundamental difference between the Kimbark curve of an individual machine and that of the equivalent OMIB system as in the IEEAC method and

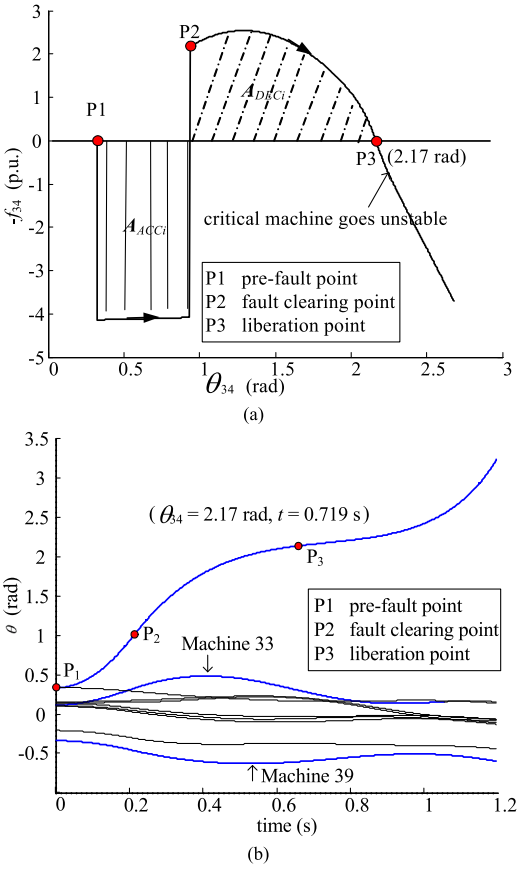

FIGURE 4. Simulations of the fault [TS-1, bus-34, 0.202s]. (a) Kimbark curve of Machine 34. (b) System trajectory.

the SIME method. In addition, some mistakes in [15] and [16] are also corrected.

III. KIMBARK CURVE OF AN INDIVIDUAL MACHINE

A. KIMBARK CURVE OF AN UNSTABLE CRITICAL MACHINE

Based on numerical simulations, the representative Kimbark curve of a critical machine becoming unstable is shown in Fig. 5(a). The corresponding system trajectory is shown in Fig. 5(b). Machines 33, 34 and 39 are critical machines for the fault [TS-1, bus-34, 0.219s].

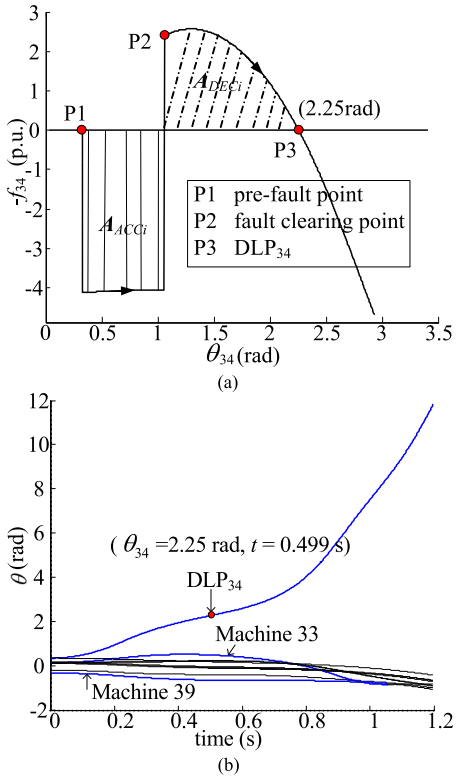

FIGURE 5. Simulations of the fault [TS-1, bus-34, 0.219s]. (a) Kimbark curve of Machine 34. (b) System trajectory.

It can be seen from Fig. 5(a) that a critical machine first accelerates from P1 to P2 during the fault-on period and then decelerates from P2 to P3 after the fault is cleared. Once the system trajectory goes through P3, the critical machine will accelerate in the COI reference and will then separate from the system. Thus, P3 can be defined as the dynamic liberation point (DLP) of this unstable critical machine [15].

Specifically, some critical machines may show negative velocities after fault clearing and finally anti-accelerate with time. In this case, the Kimbark curve of the critical machine would appear to be ''rotated'', as shown in Fig. 6 (a).

It can be seen from Figs. 4-6 that the unstable case of the critical machine can be characterized by the occurrence of the DLP with f_i of the machine being zero

$$\tilde{\omega}_i \neq 0, \quad f_i = 0 \tag{11}$$

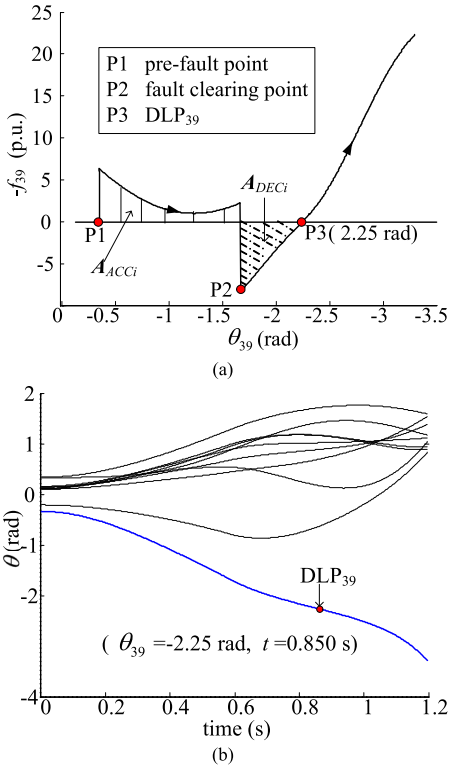

FIGURE 6. Simulations of the fault [TS-1, bus-3, 0.580s]. (a) Kimbark curve of Machine 39. (b) System trajectory.

Eq. (11) corrects the instability characterization of the critical machine in [15], [16] because these two studies neglected the anti-accelerating case as shown in Fig. 6(a).

Following IMEAC, for an unstable critical machine, we have

$$A_{ACCi} > A_{DECi} \tag{12}$$

where

$$A_{ACCi} = -\int_{\theta_i^0}^{\theta_i^c} \left[-f_i^{(F)}\right] d_{\theta_i} = \frac{1}{2} M_i \tilde{\omega}_i^{(c)2}$$

$$A_{DECi} = \int_{\theta_i^c}^{\theta_i^{DLP}} \left[-f_i^{(PF)}\right] d_{\theta_i}$$

Notice that *only* the mismatch (f_i) of machine i is zero, while mismatch values of the other machines are not zero at DLP_i. For the case that more than one critical machine becomes unstable after fault clearing, each critical machine corresponds to its unique DLP.

From analysis above, the Kimbark curve of an unstable critical machine has a clear ''accelerating-decelerating-accelerating'' characteristic. Since the Kimbark curve is formulated from actual simulated system trajectory, the Kimbark curve of an unstable critical machine and its corresponding DLP varies with the change of the faults. For instance, DLP_{34} in Fig. 4(a) is different from that in Fig. 5(a) if the system is subject to a different fault.

According to the above analysis, the Kimbark curve of an individual machine in the proposed method is somewhat similar to that of the OMIB system as in the IEEAC method and the SIME method. However, we emphasize that the EAC in the proposed method is based strictly on the Kimbark curve of an individual machine in the COI reference, which is quite different from that in the IEEAC method and the SIME method that is based on the equivalent OMIB system formed by the two groups of machines in a multi-machine system.

B. KIMBARK CURVE OF A STABLE CRITICAL MACHINE

The representative Kimbark curves of stable critical machines obtained by simulations are shown in Figs. 7(a-c). The system trajectory is shown in Fig. 7(d). Machines 33, 34 and 39 are the critical machines for the fault [TS-1, bus-34, 0.180s].

It can be seen from Figs. 7(a-c) that for a stable critical machine, the machine first accelerates from P1 to P2 during the fault-on period and then decelerates, and the velocity of the machine then reaches zero at P3. Therefore, the machine never goes through the DLP, i.e., $-f_i$ will not intersect with the horizontal zero line. Instead, $-f_i$ may turn upward or turn downward. Thus, the critical machine will not separate from the system and is maintained in a stable state in the first swing, so that P3 with zero velocity and the maximum angle can be defined as the dynamic stationary point (DSP) of the critical machine.

From analysis above, the stable case of the critical machine can be characterized by the occurrence of the DSP with the velocity of the machine equal to zero:

$$\tilde{\omega}_i = 0, \quad f_i \neq 0 \tag{13}$$

Eq. (13) corrects the stability characterization of the critical machine in [15] and [16] because these two studies neglected the anti-accelerating case as in Fig. 7(c).

Following IMEAC, when a critical machine is stable, we have:

$$A_{ACCi} = A_{DECi} \tag{14}$$

where

$$A_{DECi} = \int_{\theta_i^c}^{\theta_i^{DSP}} \left[-f_i^{(PF)}\right] d_{\theta_i}$$

In the Kimbark curve of the stable critical machine, the DSP is the inflection point where $-f_i$ turns upward or downward. The DSP describes the first swing stability of a critical machine. At the DSP of the stable critical machine i, *only* the velocity of the critical machine i is zero, while the velocities of other machines are nonzero. For the case where two or more critical machines are stable after the fault clearing, each critical machine corresponds to its unique DSP. The Kimbark curve of a stable critical machine has a clear "accelerating-decelerating" characteristic before the occurrence of the DSP, and the DSP of a stable critical machine will vary with the changes of the faults.

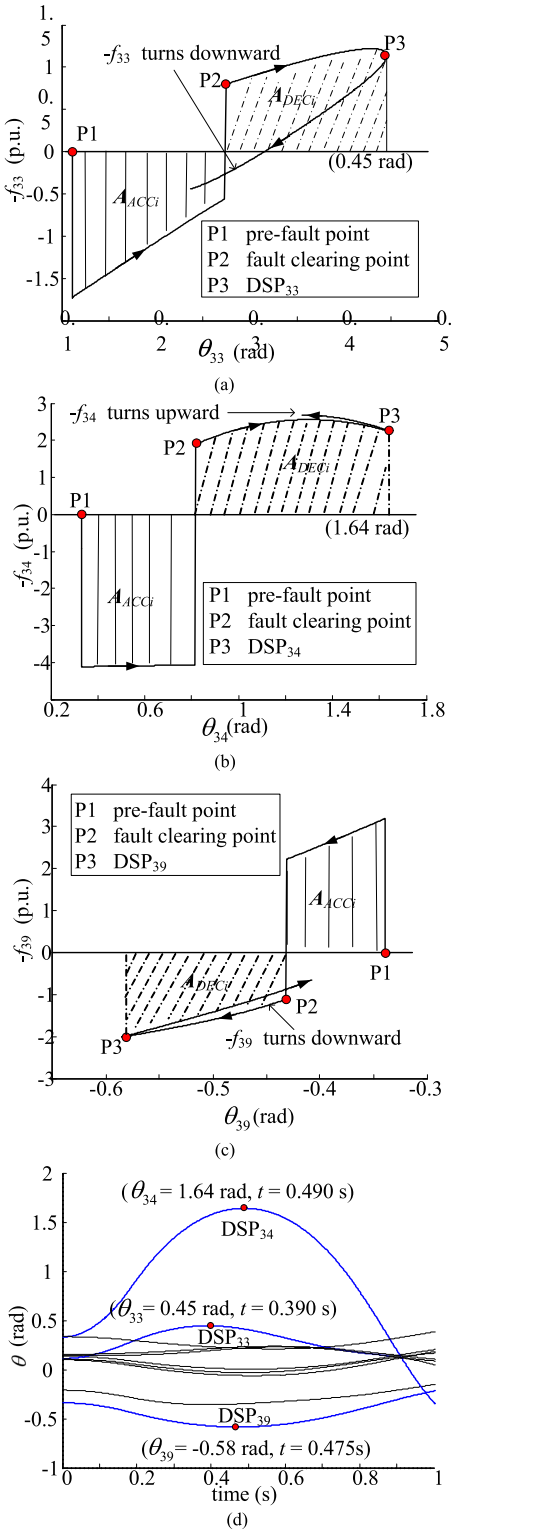

FIGURE 7. Simulations of the fault [TS-1, bus-34, 0.180s]. (a-c) Kimbark curves of Machines 33, 34 and 39. (d) System trajectory.

C. KIMBARK CURVE OF A CRITICAL-STABLE CRITICAL MACHINE

Following the stable and unstable characterization of a critical machine, once the critical machine is critically stable, the

machine is still "stable" and $-f_i$ will inflect at the DSP of the critical stable machine (CDSP). However, the CDSP is special because it just falls on the zero horizontal line, which describes the critically stable state of the machine. Therefore, the critical stable case of a critical machine is characterized by

$$\tilde{\omega}_i = 0, \quad f_i = 0 \tag{15}$$

The Kimbark curve of a critical stable machine and the corresponding system trajectory are shown in Figs. 8(a) and (b), respectively. In this case, Machine 34 is critically stable while Machines 33 and 39 are stable.

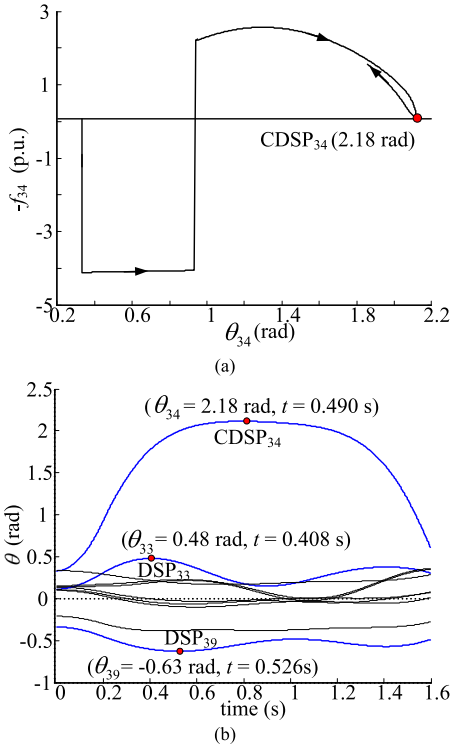

FIGURE 8. Simulations of the fault [TS-1, bus-34, 0.201s]. (a) Kimbark curve of the Machine 34. (b) System trajectory.

D. KIMBARK CURVE OF A NON-CRITICAL MACHINE

Since non-critical machines are the majority of the machines that are slightly disturbed by faults, the non-critical machines generally maintain synchronism during the post-fault period. In other words, the non-critical machines may oscillate with time, and the Kimbark curves of the non-critical machines do not show a clear "accelerating-decelerating" behavior unlike the critical machines.

The distinctive feature of the Kimbark curve of the critical machine reveals the potential of using IMEAC in the evaluation of the stability of a critical machine. Therefore, the most crucial task for the multi-machine transient stability analysis is to describe the relationship between the stability of the system and that of the critical machines, which will be analyzed in the following sections.

IV. MAPPING BETWEEN TRAJECTORY AND KIMBARK CURVE OF AN INDIVIDUAL MACHINE

A. INDIVIDUAL MACHINE TRAJECTORY

Theoretically, the transient stability of the system should be explicitly expressed as the transient stability of the "system trajectory". If a system becomes unstable, the separation of the machines in the system would occur along the time horizon. In this paper, the variation of the rotor angle of an individual machine along the time horizon is defined as the "individual-machine trajectory" (IMT). The results of a sample simulation for demonstrating the system trajectory and IMTs are shown in Figs. 9 and 10. Machines 37, 38 and 39 are the critical machines in this case.

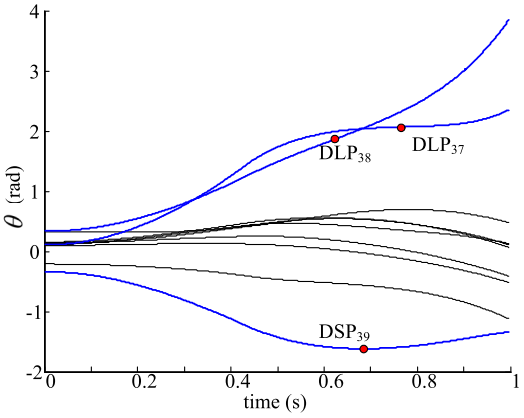

FIGURE 9. Rotor angles of the system [TS-1, bus-2, 0.430s].

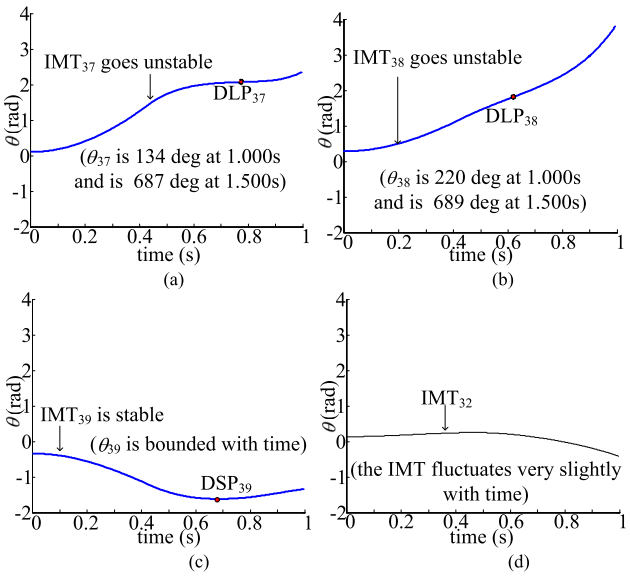

FIGURE 10. IMTs of individual machines [TS-1, bus-2, 0.430s]. (a-d) IMTs of Machines 37, 38, 39 and 32.

The IMTs in Fig. 10 reveal a commonly observed phenomenon in the power transient stability, i.e., after fault clearing, the IMTs of the critical machines fluctuate most severely, and they are most likely to separate from the system.

Comparatively, the IMTs of the non-critical machines fluctuate slightly and these machines hardly separate from the system.

Depicting the variation of the IMT in a mathematical form, the IMT of a critical machine becoming unstable is identical to the rotor angle of the machine in the COI reference becoming infinite with time, which can be expressed as

$$|\theta_{i,t}| = \left| \int_{t_0}^{t} \tilde{\omega}_i d_t \right| = +\infty \quad t = +\infty \tag{16}$$

Comparatively, the stable IMT of a critical machine is identical to the rotor angle of the machine in COI reference being bounded with time, which can be denoted as

$$|\theta_{i,t}| = \left| \int_{t_0}^{t} \tilde{\omega}_i d_t \right| < \theta_i^{bound} \quad t \in (0, +\infty) \tag{17}$$

In Eq. (17), θ_i^{bound} is the upper boundary of $\theta_{i,t}$.

Based on the analysis above, the original consideration of the trajectory stability of the system can be described as follows

(i) If the IMTs of all critical machines are bounded, the separation of machines in the system is impossible, and the system can maintain the stable state.

(ii) If the IMTs of some critical machines become infinite with time, the separation of machines in the system is certain to occur, and the system would become unstable (Figs. 10(a,b)).

(iii) The IMTs of the non-critical machines always fluctuate slightly and they hardly separate from the system, so that the IMTs of the non-critical machines cannot cause the system to become unstable (Fig. 10 (d)).

The statements above can be seen as the foundation of the proposed method. Based on the angle of the trajectory stability, the slight fluctuations of the IMTs of the non-critical machines have no effect on the instability of the system. By contrast, the severely fluctuating IMTs of the critical machines are most likely to become infinite and cause the system to become unstable. Therefore, the following criterion is proposed for TSA:

"The system operator may only monitor stability of the IMTs of critical machines during post-fault transient period.

Furthermore, the prime objective of the system operator is to determine the IMTs of unstable critical machines among all critical machines in the system because only the IMTs of unstable critical machines may cause system to become unstable."

B. 3-DIMENSIONAL KIMBARK CURVE OF A CRITICAL MACHINE

In transient stability analysis, a significant defect of observing the IMT is that it is quite difficult to describe the transient behavior of the machine. To solve this problem, it is necessary to map the stability analysis of the IMT in the $t - \theta_i$ space to the $\theta_i - f_i$ space where IMEAC can be then used to analyze the individual-machine stability.

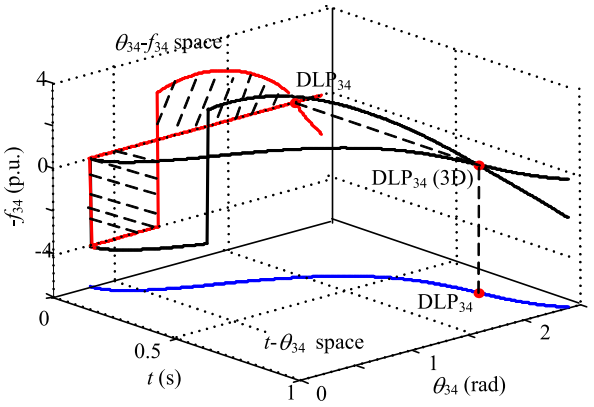

FIGURE 11. 3DKC of an unstable critical machine in a multi-machine system [TS-1, bus-34, 0.202s].

To demonstrate the mapping between IMT and IMEAC, a 3-dimensional Kimbark curve (3DKC) of a critical machine in the $t - \theta_i$–f_i space is proposed in this paper, as shown in Fig. 11. All parameters in the 3DKC of the machine are fully formulated from the actual simulated system trajectory.

It can be seen from Fig. 11 that by using the 3DKC of the critical machine, the IMT of the critical machine in the $t - \theta_i$ space is mapped to the Kimbark curve of the machine in the $\theta_i - f_i$ space, and the stability of a critical machine can be easily measured by the occurrence of the DLP or DSP in the Kimbark curve of this machine. This proves that *the stability of the IMT of a critical machine can be identified via IMEAC*.

We extend the concept of the 3DKC of an individual machine to the stability evaluation of a system with n machines. Following the definition of IMT, it is obvious that the system trajectory can be seen as the "set" that consists of IMTs of all individual machines in the system. The mappings between the system trajectory and the 3DKCs of all individual machines in the system are shown in Fig. 12.

Fig. 12 intuitively demonstrates the mechanism of using IMEAC for TSA. It can be seen from the figure that the system trajectory consists of n IMTs and each machine's IMT corresponds to its unique 3DKC; thus, the system trajectory can be easily mapped into n 3DKCs. Among all 3DKCs, considering that only the IMTs of the critical machines may cause the instability of the system, the system operator only needs to observe the 3DKCs of the critical machines by neglecting the 3DKCs of the non-critical machines. Inside the 3DKC of each critical machine, the stability of the machine is evaluated via IMEAC (i.e., the occurrence of the DLP or DSP). Once one or more critical machines are found to become unstable, the system can be determined to be unstable according to the trajectory stability theory.

V. UNITY PRINCIPLE

A. ONLY-ONE-MACHINE MONITORING

Based on the analysis described in Section IV, since the instability of the system is determined by the IMTs of the unstable critical machines, the system operators can monitor the IMT of each critical machine in the system in parallel

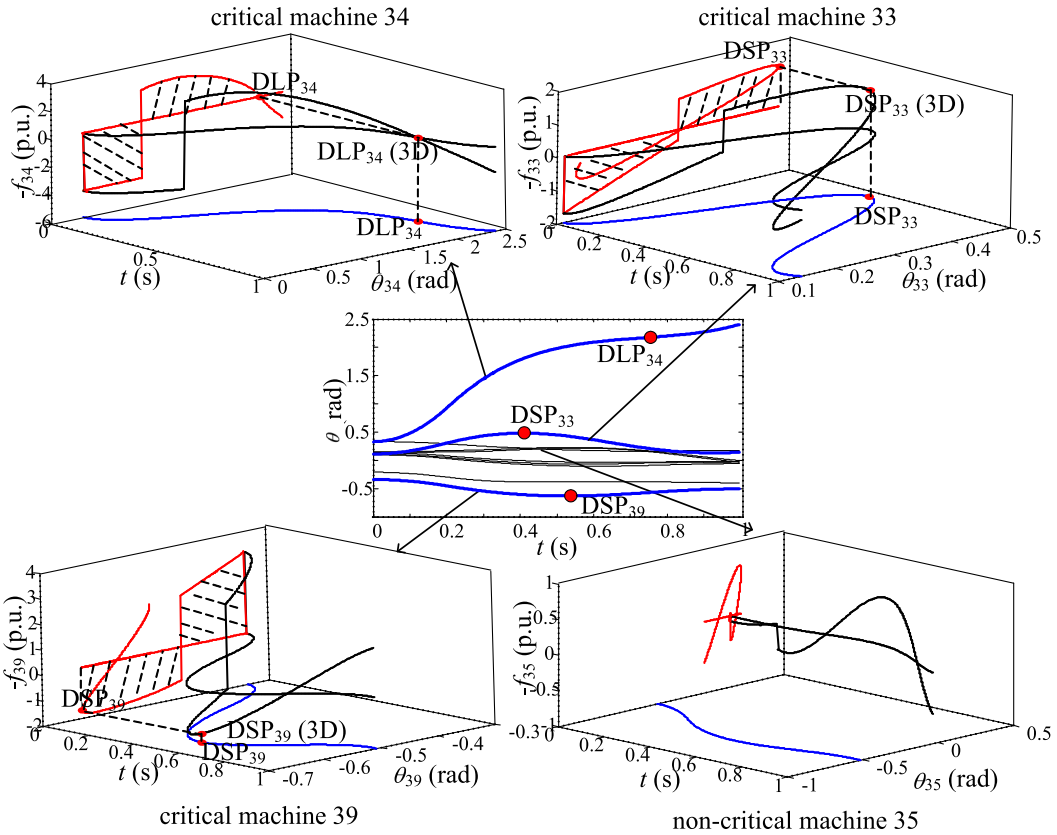

FIGURE 12. Mappings between system trajectory and 3DKCs of all individual machines in the system [TS-1, bus-34, 0.202s].

to identify the real unstable critical machine. This leads to the emergence of the following question: could the instability of the system be evaluated if the system operator does *not* monitor all critical machines?

We extend the trajectory monitoring to an extreme "only-one-machine" approach. Taking the case in Fig. 10 as an example, one can find that the IMTs of critical machines 37 and 38 both become unstable. Assume that in an extreme case, the system operator does know that ten machines are operating in the system. However, he *only* focuses on Machine 37 and does *not* observe all the other machines in the system, as shown in Fig. 13. In this extreme "only-one-machine-monitoring" case, could the system still be defined as unstable?

From Fig. 13, one can see that in the COI reference, DLP_{37} occurs at 0.776 s and θ_{37} reaches 687 deg. at 1.500 s. In this extreme "only-one-machine monitoring" case, although the IMTs of all the other machines in the system are not monitored, it is quite obvious that the system cannot be maintained in a stable state because IMT_{37} keeps separating from the system with time.

Theorem: Transient instability of any one IMT determines the transient instability of the system trajectory.

Proof: Using reductio ad absurdum, assume that the system is stable when an IMT in the system already becomes infinite with time. Following the trajectory stability theory, this assumption contradicts the sufficient and necessary

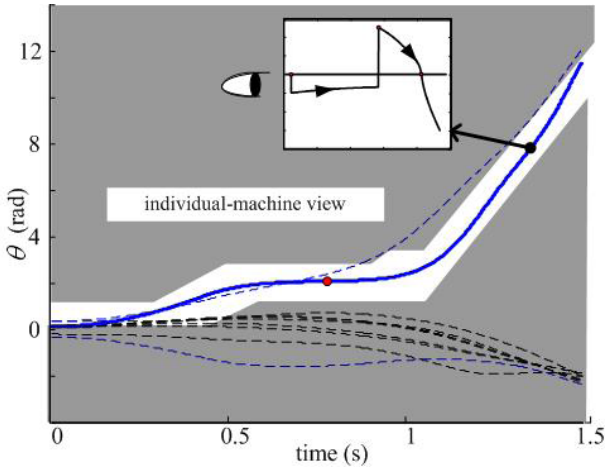

FIGURE 13. Monitoring IMT of only one unstable machine [TS-1, bus-2, 0.430s].

condition for the maintenance of the system stability, i.e., the IMTs of all machines in the system should be bounded along the time horizon (Section IV); thus, the theorem holds.

Following the analysis above, the unity of the individual-machine stability and system stability can be expressed as follows:

(I) The system can be considered to be stable if all critical machines are stable.

(II) The system can be considered to be unstable as long as any one critical machine is found to become unstable.

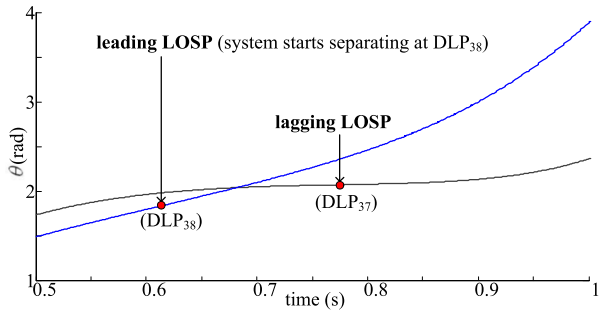

FIGURE 14. Multiple LOSPs in a multimachine system [TS-1, bus-2, 0.430s].

Principles I and II substantially illustrate the unity of the individual-machine stability and system stability. Principle II is of particular interest because it reflects the fact that the transient stability of a multi-machine system may be monitored in an individual-machine manner, and the instability of the system can be determined by any one unstable critical machine without monitoring all critical machines in the system. This provides a quite novel individual-machine approach for the transient stability analysis in TSA.

B. OCCURRENCE OF MULTIPLE LOSPS OF THE SYSTEM

Following the unity principle, since each unstable critical machine may cause the system to become unstable, the DLP of each unstable critical machine can be seen as the loss-of-synchronism point (LOSP) of the system. Therefore, multiple LOSPs may exist along the post-fault system trajectory if more than one critical machine becomes unstable. These LOSPs can be defined as follows:

Leading LOSP: The leading LOSP is defined as the first occurred DLP along the time horizon;

Lagging LOSP: The lagging LOSP is defined as the DLP that occurs later than the leading LOSP.

Based on the above definitions, the system can be considered as unstable once the leading LOSP or the lagging LOSPs are monitored. However, the leading LOSP is certainly the most valuable for the system operators because the system starts separating at this point, as shown in Fig. 14.

C. MACHINE-BY-MACHINE STABILITY EVALUATION

From the analysis above, it can be seen that in an actual TSA environment, the system operator may monitor each critical machine in parallel once the fault is cleared, and the stability of a critical machine can be identified once the corresponding DLP or DSP occurs in the Kimbark curve. However, since the DSPs and DLPs occur one after another along the post-fault system trajectory as analyzed in Section II, the stability of the critical machines in the system can only be identified in a ''machine-by-machine'' manner along the time horizon. Furthermore, during this process the system can be evaluated as unstable immediately once the leading LOSP occurs without waiting for the stability evaluations of the rest of the critical machines. A tutorial example will be provided in the next section to demonstrate the application of the IMEAC in TSA.

VI. A TUTORIAL EXAMPLE

A. PARALLEL MONITORING

The case [TS-1, bus-2, 0.430s] is provided here to demonstrate the machine-by-machine stability evaluation when using the proposed method in TSA. The simulated system trajectory is shown in Fig. 15.

In Fig. 15, once the fault is cleared, Machines 37, 38 and 39 are identified as the critical machines. Therefore, the system operator monitors the IMTs of these three critical machines in parallel by neglecting that of the non-critical machines. Along the time horizon, the system operator focuses especially on the following points in time.

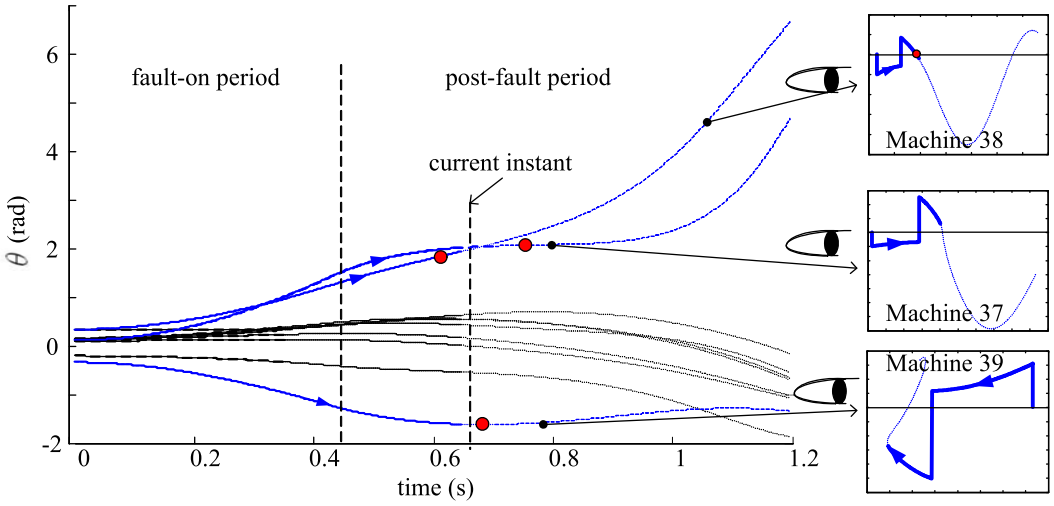

FIGURE 15. Demonstration of parallel monitoring [TS-1, bus-2, 0.430s].

DLP_{38} occurs (0.614 s): Machine 38 is evaluated as unstable.

DSP_{39} occurs (0.686 s): Machine 39 is evaluated as stable.

DLP_{37} occurs (0.776 s): Machine 37 is evaluated as unstable.

The stability of the system is determined as follows:

DLP_{38} occurs (0.614 s): DLP_{38} is defined as leading LOSP, and the system is considered to be unstable.

DLP_{37} occurs (0.776 s): DLP_{37} is defined as lagging LOSP, yet the system has already been unstable for a while.

From the analysis above, DLP_{38} and DLP_{37} are the leading LOSP and lagging LOSP, respectively. f_i of all machines in the system at the instant of the occurrence of DLP_{37} (0.776 *s*) are shown in Table 1.

TABLE 1. Acceleration power of machines at DLP_{37}.

No.	f_i (p.u.)	Machine num	f_i (p.u.)
37	0.00	32	0.77
38	-2.48	33	0.04
39	-3.59	34	1.14
30	1.53	35	1.31
31	0.55	36	0.70

It can be seen from Table 1 that at 0.776 *s* only f_{37} is zero, while f_i of other machines are not zero so that DLP_{37} is only the acceleration point for Machine 37, which is meaningless for the stability evaluation of the other critical machines in the system.

B. ONLY-ONE-MACHINE MONITORING

For the case given in Fig. 15, assume that the system operator monitors only one critical machine and does not monitor the other two critical machines. Under these circumstances, three different cases are shown as follows:

1) ONLY MACHINE 38 IS MONITORED

In this case, the system can be considered to be unstable by only monitoring the unstable Machine 38 via the unity principle, and the leading LOSP is obtained.

2) ONLY MACHINE 37 IS MONITORED

In this case, the system can also be evaluated as unstable by only monitoring the unstable Machine 37. However, the leading LOSP cannot be obtained. Only the lagging LOSP is obtained.

3) ONLY MACHINE 39 IS MONITORED

In this case, the system operator cannot evaluate whether the system is stable or not by only monitoring the stable Machine 39, thus the rest of the critical machines still need to be monitored to finally confirm the instability of the system.

The individual-machine monitoring cases above indicate that each critical machine's ''status'' for transient stability analysis in the system is different, and this will be analyzed in the companion paper.

VII. CONCLUSIONS

Through the analysis presented in this paper, the following conclusions can be reached:

(i) EAC is proved to strictly hold for a critical machine. The Kimbark curve of a critical machine exhibits a strong ''accelerating-decelerating'' behavior.

(ii) The critical machines are most likely to separate from the system, and the system operator may only focus on analyzing the stability of the critical machines.

(iii) A critical machine becoming unstable in $\theta_i - f_i$ space is identical to the IMT of the critical machine becoming unstable in $t - \theta_i$ space.

(iv) The unity principle indicates that monitoring of the transient stability of the multi-machine system can be treated in an individual-machine approach, and the transient instability of the multi-machine system can be determined by the evaluation for any one unstable critical machine.

In the companion paper, the application of the IMEAC and individual-machine stability evaluation will be analyzed, which may demonstrate the effectiveness of the proposed method in TSA.

REFERENCES

[1] A. A. Fouad, ''Transient stability criteria,'' in *Proc. IEEE Conf. Decision Control Including 14th Symp. Adapt. Process.*, Houston, TX, USA, 1975, pp. 309–314.

[2] J. Shu, W. Xue, and W. Zheng, ''A parallel transient stability simulation for power systems,'' *IEEE Trans. Power Syst.*, vol. 20, no. 4, pp. 1709–1717, Nov. 2005.

[3] I. Nagel, L. Fabre, M. Pastre, F. Krummenacher, R. Cherkaoui, and M. Kayal, ''High-speed power system transient stability simulation using highly dedicated hardware,'' *IEEE Trans. Power Syst.*, vol. 28, no. 4, pp. 4218–4227, Nov. 2013.

[4] G. Hou and V. Vittal, ''Determination of transient stability constrained interface real power flow limit using trajectory sensitivity approach,'' *IEEE Trans. Power Syst.*, vol. 28, no. 3, pp. 2156–2163, Aug. 2013.

[5] B. Sapkota and V. Vittal, ''Dynamic VAr planning in a large power system using trajectory sensitivities,'' *IEEE Trans. Power Syst.*, vol. 25, no. 1, pp. 461–469, Feb. 2010.

[6] Y. Li and Z. Yang, ''Application of EOS-ELM with binary Jaya-based feature selection to real-time transient stability assessment using PMU data,'' *IEEE Access*, vol. 5, pp. 23092–23101, 2017.

[7] T. Athay, R. Podmore, and S. Virmani, ''A practical method for the direct analysis of transient stability,'' *IEEE Trans. Power App. Syst.*, vol. PAS-98, no. 2, pp. 573–584, Mar. 1979.

[8] N. Kakimoto, Y. Ohsawa, and M. Hayashi, ''Transient stability analysis of electric power via lure type Lyapunov function, part I new critical value for transient stability,'' *IEE Trans. Jpn.*, vol. 98, nos. 5–6, pp. 63–71, 1978.

[9] T. Odun-Ayo and M. L. Crow, ''Structure-preserved power system transient stability using stochastic energy functions,'' *IEEE Trans. Power Syst.*, vol. 27, no. 3, pp. 1450–1458, Aug. 2012.

[10] A. A. Fouad and S. E. Stanton, ''Transient stability of a multi-machine power system. Part I: Investigation of system trajectories,'' *IEEE Trans. Power App. Syst.*, vol. PAS-100, no. 7, pp. 3408–3416, Jul. 1981.

[11] A. A. Fouad and S. E. Stanton, ''Transient stability of a multi-machine power system. Part II: Critical transient energy,'' *IEEE Trans. Power App. Syst.*, vol. PAS-100, no. 7, pp. 3417–3424, Jul. 1981.

[12] V. Vittal, ''Power system transient stability using the critical energy of individual machines,'' Ph.D dissertation, Dept. Elect. Comput. Eng., Iowa State Univ., Ames, IA, USA, 1982.

[13] A. Michel, A. Fouad, and V. Vittal, ''Power system transient stability using individual machine energy functions,'' *IEEE Trans. Circuits Syst.*, vol. CAS-30, no. 5, pp. 266–276, May 1983.

[14] S. E. Stanton, ''Assessment of the stability of a multimachine power system by the transient energy margin,'' Ph.D dissertation, Dept. Elect. Comput. Eng., Iowa State Univ., Ames, IA, USA, 1982.

[15] S. E. Stanton and W. P. Dykas, "Analysis of a local transient control action by partial energy functions," *IEEE Trans. Power Syst.*, vol. 4, no. 3, pp. 996–1002, Aug. 1989.
[16] S. E. Stanton, "Transient stability monitoring for electric power systems using a partial energy function," *IEEE Trans. Power Syst.*, vol. 4, no. 4, pp. 1389–1396, Nov. 1989.
[17] S. E. Stanton, C. Slivinsky, K. Martin, and J. Nordstrom, "Application of phasor measurements and partial energy analysis in stabilizing large disturbances," *IEEE Trans. Power Syst.*, vol. 10, no. 1, pp. 297–306, Feb. 1995.
[18] P. Rastgoufard, A. Yazdankhah, and R. A. Schlueter, "Multi-machine equal area based power system transient stability measure," *IEEE Trans. Power Syst.*, vol. PWRS-3, no. 1, pp. 188–196, Feb. 1988.
[19] M. H. Haque, "Further developments of the equal-area criterion for multimachine power systems," *Electr. Power Syst. Res.*, vol. 33, pp. 175–183, Jun. 1995.
[20] R. Ando and S. Iwamoto, "Highly reliable transient stability solution method using energy function," *IEEE Trans. Jpn.*, vol. 108, no. 4, pp. 57–66, 1988.

SONGYAN WANG received the B.S., M.S., and Ph.D. degrees from the School of Electrical Engineering and Automation, Harbin Institute of Technology (HIT), in 2007, 2009, and 2012, respectively. He was a Visiting Scholar at Virginia Tech, Blacksburg, VA, USA, in 2010. From 2013 to 2014, he was a Research Fellow with Queen's University Belfast, U.K. He is currently an Assistant Professor with HIT. His research interests include power system operation and control.

Dr. Wang is an Associate Editor of the *Renewable and Sustainable Energy Reviews*.

JILAI YU joined the School of Electrical Engineering and Automation, Harbin Institute of Technology, in 1992. From 1994 to 1998, he was an Associate Professor with the School of Electrical Engineering and Automation, Harbin Institute of Technology, where he is currently a Professor and the Director of the Electric Power Research Institute. His current research interests include power system analysis and control, optimal dispatch of power system, green power, and smart grid.

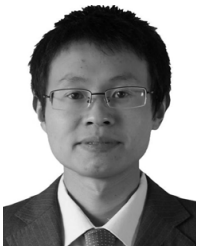

WEI ZHANG (S'11–M'14) received the B.S. and M.S. degrees in power system engineering from the Harbin Institute of Technology, Harbin, China, in 2007 and 2009, respectively, and the Ph.D. degree in electrical engineering from New Mexico State University, Las Cruces, NM, USA, in 2013.

He is currently an Associate Professor with the School of Electrical Engineering and Automation, Harbin Institute of Technology. His research interests include distributed control and optimization of power systems, renewable energy and power system state estimation, and stability analysis.